

# Effects of $\gamma/\gamma$ interfacial structures on continuous coarsening of lamellar microstructure in TiAl alloy during aging<sup>①</sup>

LI Zhen-xi(李臻熙), CAO Chun-xiao(曹春晓)  
(Beijing Institute of Aeronautical Materials, Beijing 100095, China)

**Abstract:** The effects of  $\gamma/\gamma$  interfacial structures on continuous coarsening of the fully lamellar microstructure in Ti-48Al alloy aged at 1 150 °C were investigated by using transmission electron microscopy (TEM). Continuous lamellar coarsening can be achieved not only by migration of interface faults (such as ledges, edges and curved interfaces) but also by migration and decomposition of perfect  $\gamma/\gamma$  lamellar interfaces. Thermal grooves, initiative positions of interfacial dissociation, can frequently form at the triple point junctions between the 120°-rotational ordered  $\gamma$  domain boundaries within  $\gamma$  lamellae and the lamellar interfaces. During the early stage of aging at 1 150 °C, the interface migration and dissociation took place preferentially at the 120°-rotational ordered lamellar interfaces. Comparing the relative thermal stability of the true-twin, pseudo-twin and 120°-rotational ordered  $\gamma/\gamma$  lamellar interfaces shows that the 120°-rotational ordered lamellar interface is the most unstable. The reason of this phenomenon was analyzed through the comparisons of the interfacial energies and atomic arrangements of the three types of  $\gamma/\gamma$  lamellar interfaces.

**Key words:** titanium aluminide; lamellar microstructure; continuous coarsening;  $\gamma/\gamma$  lamellar interface; orientation relationship; aging

**CLC number:** TG 146

**Document code:** A

## 1 INTRODUCTION

As a candidate of high temperature material for structure applications,  $\gamma$ -based titanium aluminide alloys have attracted considerable interest, especially for those with fully lamellar microstructure consisting of  $\gamma$  ( $L1_0$  structure) and  $\alpha_2$  ( $D0_{19}$  structure) lamellae. These alloys can have attractive combinations of mechanical properties, such as high creep resistance, fracture toughness and specific strength<sup>[1,2]</sup>. However, the mechanical properties of fully lamellar microstructures deteriorate when the lamellar structure becomes unstable during a long-term thermal or thermomechanical exposure<sup>[3,4]</sup>. Hence, it is very important to investigate the instability mechanisms in lamellar structures.

TiAl-based alloys are similar to other alloy systems with lamellar structures<sup>[5,6]</sup> in that continuous coarsening and discontinuous coarsening are the two main instability mechanisms. Continuous coarsening is a process of reduction in interface area through coarsening either by lattice diffusion or pipe diffusion while discontinuous coarsening is by grain boundary migration. Discontinuous coarsening has been well documented in Refs. [7-10], however, a limited number of investigations are concerned with continuous coarsening and many aspects of it have still remained ambiguous, such as the effects of the  $\gamma/\gamma$  interfacial structure.

Because the  $\langle 11\bar{0} \rangle$  and  $\langle 01\bar{1} \rangle$  directions in the  $L1_0$  structure of the  $\gamma$  phase are not equivalent crystallographically, there are three types of  $\gamma/\gamma$  lamellar interfaces defined by orientation relationships between two neighboring  $\gamma$  lamellae. When corresponding crystal orientations in two neighboring  $\gamma$  lamellae are rotated relatively by  $\pm 60^\circ$ ,  $\pm 120^\circ$  and  $\pm 180^\circ$  about the  $[111]$  direction (the normal direction to the  $\gamma/\gamma$  interface), the pseudo-twin, 120°-rotational order and true-twin  $\gamma/\gamma$  lamellar interfaces can be obtained<sup>[11,12]</sup>, respectively. Fig. 1 shows the orientation relationships of the pseudo-twin, 120°-rotational order as well as true-twin  $\gamma/\gamma$  lamellar interfaces. Because the three types of  $\gamma/\gamma$  lamellar interfaces differ in the interfacial energy and the stacking sequence on the  $\{111\}$  planes across  $\gamma/\gamma$  interface, their thermal stabilities are different. Therefore, the  $\gamma/\gamma$  lamellar interfacial structure may play a key role in the continuous coarsening of lamellar microstructure. In the present paper, the effects of  $\gamma/\gamma$  interfacial structures on the continuous coarsening of fully lamellar microstructure in Ti-48Al alloy during aging at 1 150 °C were investigated.

## 2 EXPERIMENTAL

Alloy ingots of nominal composition Ti-48% Al (mole fraction) were prepared by nonconsumable electrode arc melting. A fully lamellar microstructure

① Received date: 2003 - 04 - 15; Accepted date: 2003 - 06 - 08

Correspondence: LI Zhen-xi, PhD; Tel: + 86 10-62458116; Fax: + 86 10-62456925; E-mail: zhenxi.li@biam.ac.cn

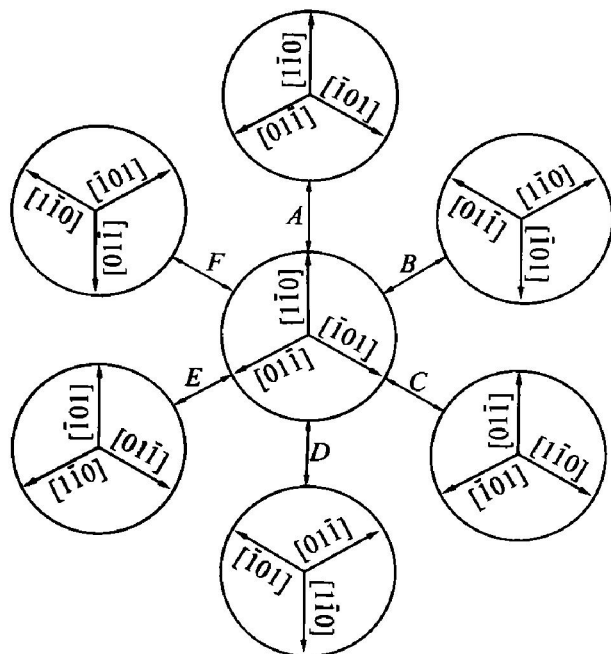


**Fig. 1** Schematic representation of orientation relationships of  $\gamma/\gamma$  lamellar interfaces  
(A: Perfect crystal; B & F: Pseudotwin relationship;  
C & E:  $120^\circ$ -rotational order relationship;  
D: True twin relationship)

was produced by heat-treatment at  $1\,400\text{ }^\circ\text{C}$  for 1 h followed by air cooling. Then the specimens of the fully lamellar microstructure were further aged at  $1\,150\text{ }^\circ\text{C}$  for 4 h in air. Microstructure evolution was analyzed by using a JEM-200CX transmission electron microscope. TEM foils were prepared by twin jet electron polish method using a solution of 59% methanol, 35% butyl cellusolve and 6% perchloric acid and operating at  $-30\text{ }^\circ\text{C}$  and 40 V.

### 3 RESULTS AND ANALYSES

Figs. 2(a) and (b) show a TEM image of fully lamellar microstructure produced by heat-treatment at  $1\,400\text{ }^\circ\text{C}$  for 1 h followed by air cooling and the corresponding SAD pattern, respectively. The primary lamellar microstructure consists of alternating several  $\gamma$  phase lamellae and single  $\alpha_2$  phase lamella. The average interlamellar spacing is about  $0.2\text{ }\mu\text{m}$ . The  $\gamma$  and  $\alpha_2$  lamellae keep the  $\{111\}_\gamma \parallel (0001)_{\alpha_2}$ ,  $\langle 110 \rangle_\gamma \parallel \langle 11\bar{2}0 \rangle_{\alpha_2}$  Blackburn orientation relationship<sup>[13]</sup> as illustrated in Fig. 2(b). Due to the high Al content in Ti-48Al alloy, the volume fraction of  $\alpha_2$  lamellae is low and the majority of lamellar interface is  $\gamma/\gamma$  lamellar interface. Thus, the thermal stability of the fully lamellar microstructure is controlled by the stability of  $\gamma/\gamma$  lamellar interfaces rather than that of  $\gamma/\alpha_2$  phase interfaces.

As shown in Fig. 2(a), the planar  $\gamma/\gamma$  and  $\alpha_2/\gamma$  lamellar interfaces are very regular and there is almost no curvature imperfection to promote volume-

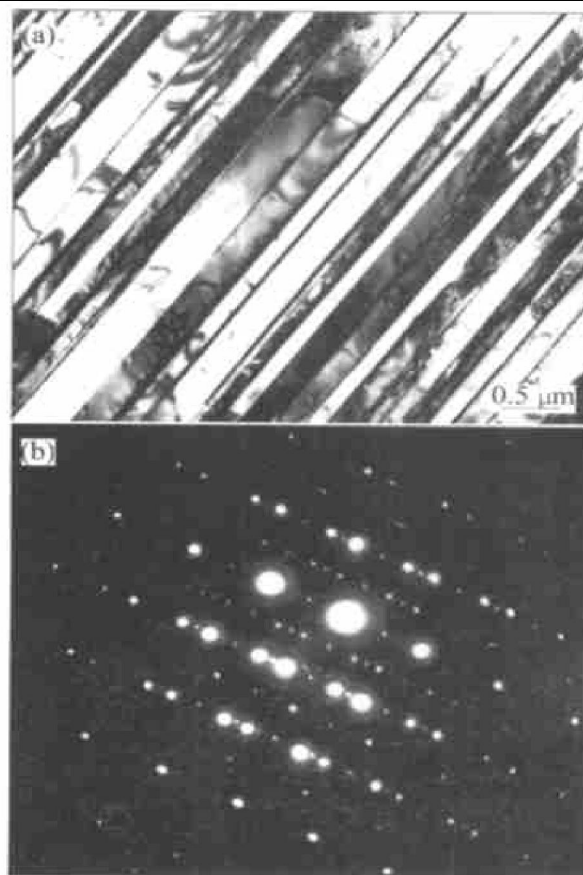


**Fig. 2** TEM image of air-cooling lamellar microstructure(a) and SAD pattern(b) with  $\mathbf{B} = [1210]_{\alpha_2} \parallel [110]_\gamma \parallel [\bar{1}10]_{\gamma_T}$

diffusion-controlled continuous coarsening. However, many kinds of interfacial faults, such as interfacial ledges, edges of terminate lamellae, curved interfaces and ordered domain boundaries, can be found under the TEM observation with higher magnification, as shown in Figs. 3(a-d) respectively. These interfacial faults play a key role in initiating instability of the primary lamellar microstructure, because the solute concentration gradient, which is the driving force for continuous coarsening of lamellar microstructure, exists between the faults and the flat interfaces according to the Gibbs-Thomson theorem.

Fig. 4(a) shows a typical TEM image of continuously coarsened lamellar structure after aging at  $1\,150\text{ }^\circ\text{C}$  for 4h. The crystallographic orientations of  $\gamma_1 - \gamma_8$  domains are identified through analysis of the corresponding SAD patterns indicated in Figs. 4(b-h). The atomic arrangement along  $\pm[110]$  direction in  $L1_0$  structure is different from that along  $\pm[011]$  and  $\pm[\bar{1}01]$  directions, the additional  $\pm(001)$  and  $\pm(110)$  superlattice diffraction spots reveal when the incident electron beam is parallel to the  $\pm[110]$  diffraction zone direction<sup>[14, 15]</sup>. Accordingly, the

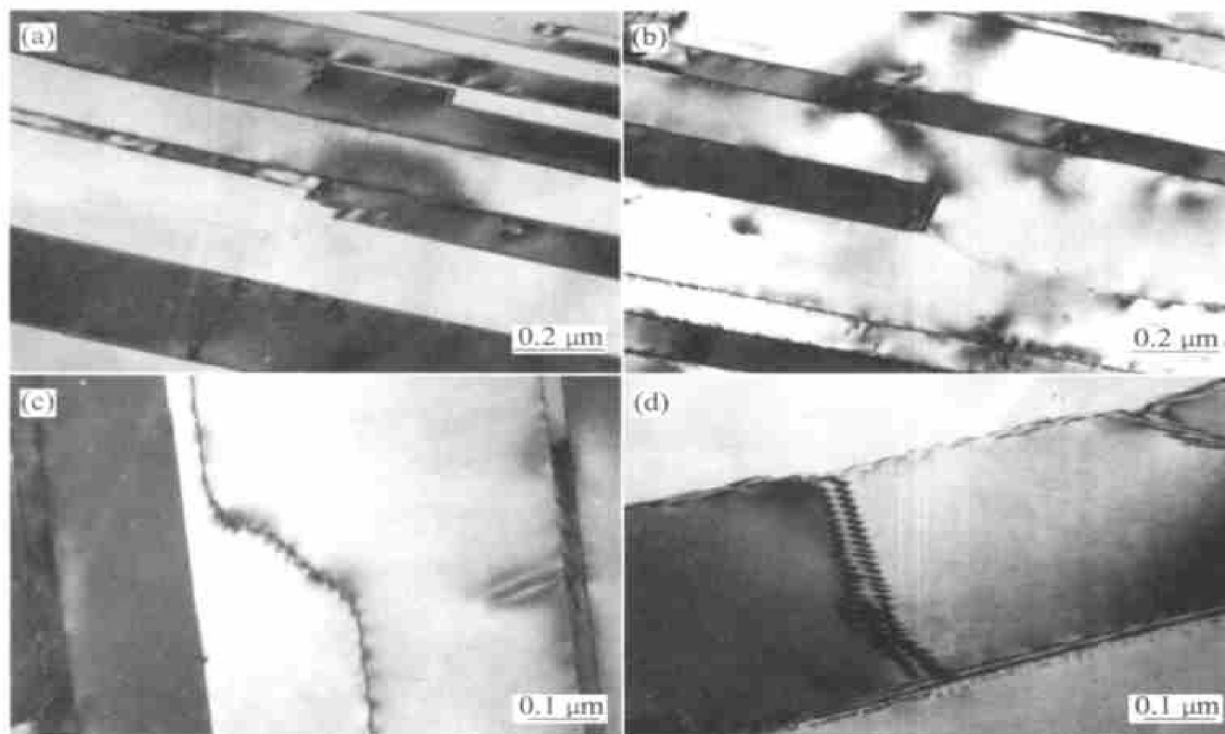


**Fig. 3** TEM images of interface faults in air-cooling lamellar microstructure  
(a) —Interface ledges; (b) —Edge of a terminate plate; (c) —Curved interface; (d) —Ordered domain boundaries

SAD pattern of  $\pm [110]$  zone direction can be easily distinguished from that of  $\pm [011]$  and  $\pm [101]$  zone directions. If the lamellar interfaces are defined as  $(111)_{\gamma} \parallel (0001)_{\alpha_2}$ , the diffraction zone directions of  $\gamma_1 - \gamma_8$  domains can be indexed as  $[110]_{\gamma_1}$ ,  $[011]_{\gamma_2}$ ,  $[101]_{\gamma_3}$ ,  $[011]_{\gamma_4}$ ,  $[101]_{\gamma_5}$ ,  $[110]_{\gamma_6}$ ,  $[101]_{\gamma_7}$ , and  $[110]_{\gamma_8}$ , respectively. According to the orientation relationships of  $\gamma/\gamma$  lamellar interfaces as illustrated in Fig. 1, the  $\gamma_2/\gamma_6$ ,  $\gamma_3/\gamma_6$ ,  $\gamma_4/\gamma_6$ ,  $\gamma_5/\gamma_6$ ,  $\gamma_7/\gamma_6$ ,  $\gamma_3/\gamma_4$  and  $\gamma_4/\gamma_5$  interfaces can be determined as  $120^\circ$ -rotational order interfaces because no twin diffraction spots occur in the corresponding SAD patterns. The  $\gamma_6/\gamma_8$  and  $\gamma_1/\gamma_6$  keep the true-twin relationship and the  $\gamma_1/\gamma_2$ ,  $\gamma_1/\gamma_3$ ,  $\gamma_1/\gamma_4$ ,  $\gamma_1/\gamma_5$  and  $\gamma_7/\gamma_8$  maintain the pseudo-twin relationship. A schematic illustration corresponding to Fig. 4(a) is shown in Fig. 4(i), and all of the  $\gamma/\gamma$  interfaces are

classified and listed in Fig. 4(i). The dashed lines in Fig. 4(i) represent the assumed original lamellar interfaces before continuous coarsening occurs.

The above analyzed results show that all of the dissociated or migrated  $\gamma/\gamma$  interfaces in Fig. 4(a) are the  $120^\circ$ -rotational order interfaces, the true-twin and pseudo-twin interfaces are very stable and no obvious variations in them are observed. This prevalent phenomenon in the aged specimen indicates that the thermal stability of  $120^\circ$ -rotational order interfaces is poor compared with that of the true-twin and pseudo-twin interfaces. It is worth noting that a thermal groove, named by Ramanujan et al.<sup>[16]</sup>, has formed at the triple point junction between the  $\gamma_1/\gamma_3$ ,  $\gamma_1/\gamma_4$  lamellar interfaces and the  $\gamma_3/\gamma_4$  domain boundary as indicated by the arrow *G* in Fig. 4(a). This thermal groove may be an initiative position of interface dissociation.

The segment *B* on the  $120^\circ$ -rotational order interface  $\gamma_1/\gamma_2$  (see the SAD patterns in Figs. 6(b, c)) bowed out from its original site. This configuration of the  $120^\circ$ -rotational order lamellar interfaces is unstable. Extending the aging time the migration of the irregular interface segments *A* and *C* will result in the dissociation of the segment *B* from the  $\gamma_1/\gamma_2$  interface.

## 4 DISCUSSION

Because the coherent or semicoherent  $\gamma/\gamma$  and  $\gamma/\alpha_2$  lamellar interfaces in the initial lamellar microstructure are very flat and there is almost no curva-

The interface dissociation starting from the thermal groove is an important mechanism of continuous coarsening. Fig. 5(a) shows a typical TEM image of dissociated lamellar interfaces in the aged specimen. The analysis of interfacial orientation relationship shown in Figs. 5(b–h) indicates that interface dissociation occurs preferentially on the  $120^\circ$ -rotational order interfaces. These interrupted  $\gamma$  lamellae can be frequently observed in the aged sample.

Another mechanism of continuous coarsening of lamellar structure is by interface migration. A typical example of interface migration is shown in Fig. 6(a).

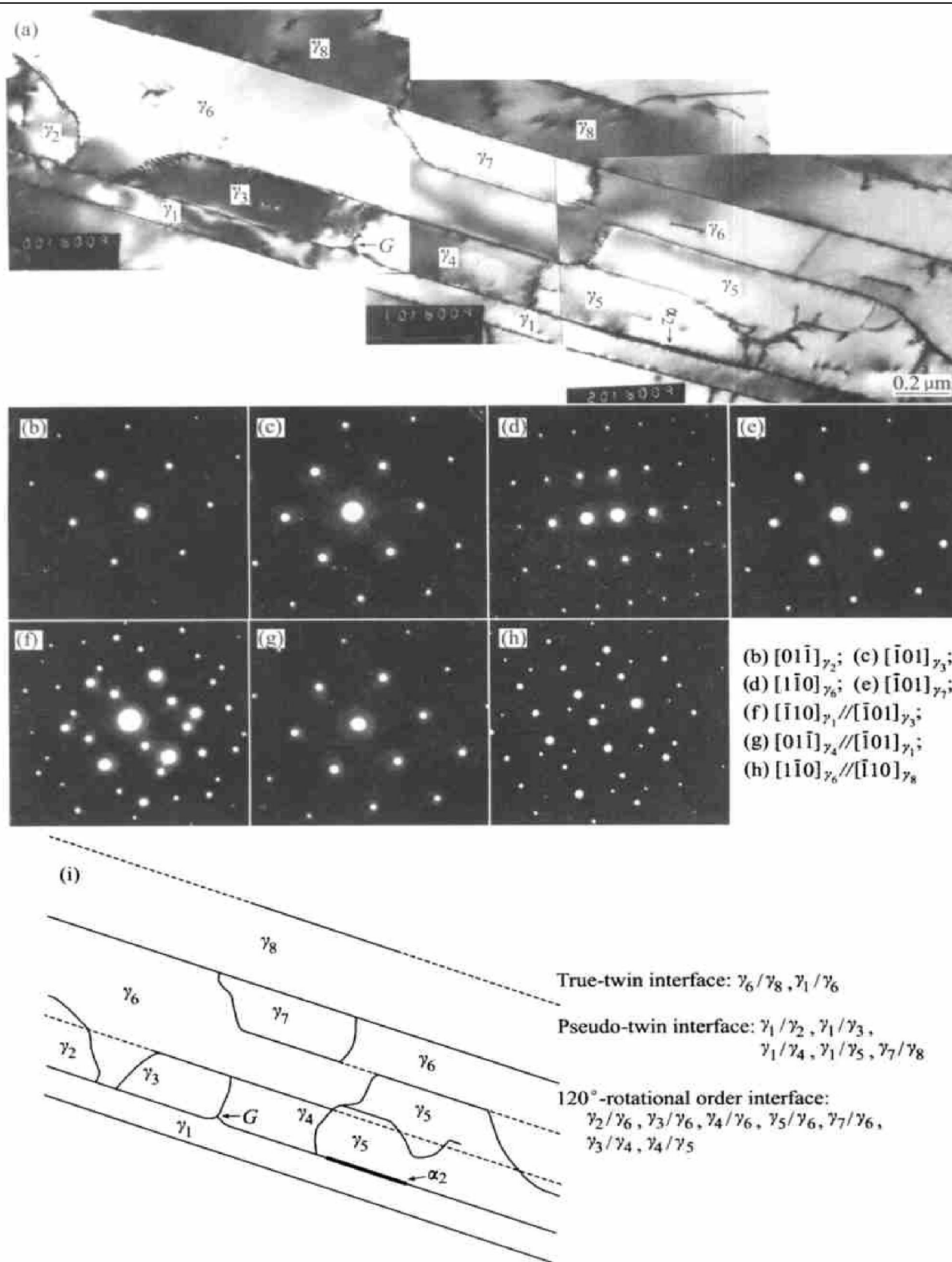


**Fig. 4** TEM image of continuous coarsening lamellar microstructure (a), SAD patterns of  $\gamma$  domains (b-h) and schematic illustration (i)

ture variation to promote continuous coarsening controlled by volume diffusion, the thermal microstructural stability, in general, is basically good. However, several kinds of interfacial defects exist in the initial lamellar microstructure (Fig. 3). According to the Gibbs-Thomson theorem, solute concentration gradient exists between interfacial defect and flat interface

due to the existence of curvature difference. During aging at high temperature, the ensuing flux of solute leads to migration of the defect, such as ledge migration and edge recession as schematically illustrated in Figs 7 (a, b), then the continuous coarsening of lamellar structure takes place.

In addition to the way of interfacial defect mi-

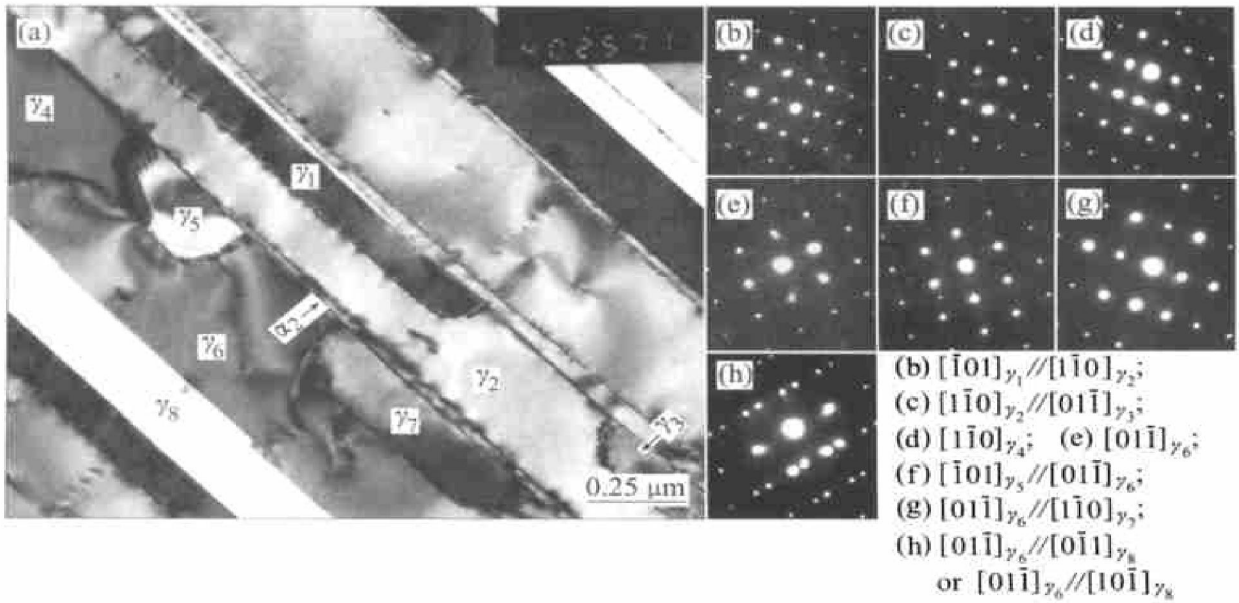


**Fig. 5** TEM image of dissociated 120°-rotational ordered lamellar interface(a)

and SAD patterns of  $\gamma$  lamellae (b - h)

Twin interface:  $\gamma_6/\gamma_8$ ; 120°-rotational order interface:  $\gamma_1/\gamma_2$ ,  $\gamma_3/\gamma_2$ ,  $\gamma_4/\gamma_6$ ,  $\gamma_5/\gamma_6$ ,  $\gamma_7/\gamma_6$

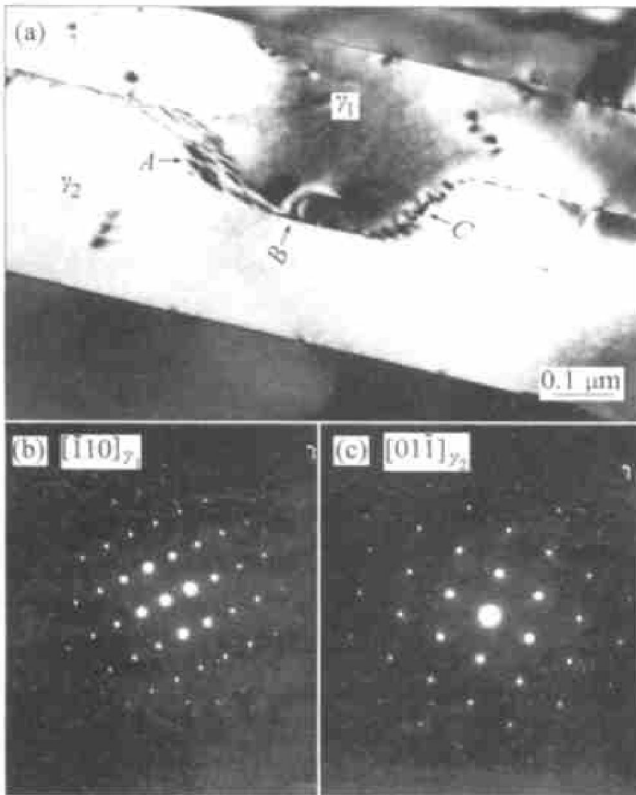


**Fig. 6** TEM image of migrated 120°-rotational ordered lamellar interface(a) and SAD patterns of  $\gamma_1$  and  $\gamma_2$  lamellae(b, c)

gration mechanism,  $\gamma/\gamma$  interface dissociation and migration are also two important mechanisms of continuous coarsening in lamellar structures. Schematic illustrations of these are shown in Figs. 7(c, d). In the present investigation, it is found that the thermal stability of 120°-rotational ordered  $\gamma/\gamma$  lamellar interface is poor compared with that of true-twin and pseudo-twin  $\gamma/\gamma$  lamellar interface, and interface

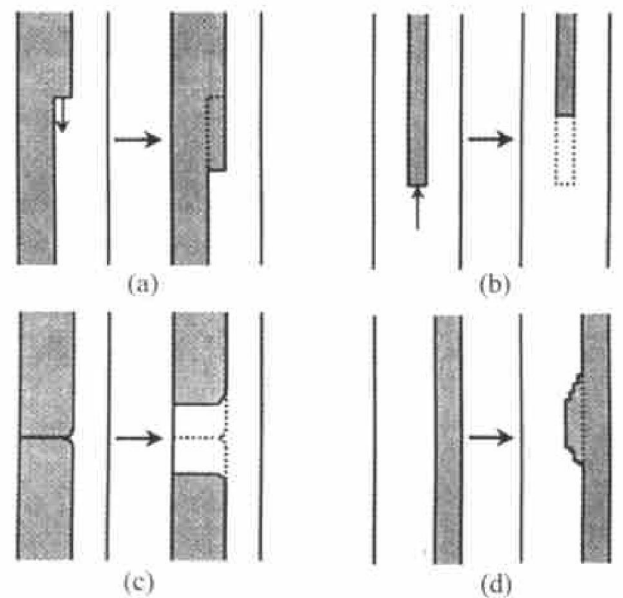


**Fig. 7** Schematic illustrations of continuous coarsening mechanism of lamellar microstructure

(a) —Ledge migration; (b) —Edge recession;  
(c) —Interface dissociation; (d) —Interface migration

dissociation or migration occur preferentially on the 120°-rotational ordered  $\gamma/\gamma$  lamellar interface. The analysis results of SAD patterns shown in Figs. 4 - 6 give the evidence for this phenomenon. The difference in two aspects of interfacial characteristic, interface energy and atomic arrangement across interface, of the three types of  $\gamma/\gamma$  interfaces can be used to explain this behavior. The ratio of interfacial energies for the true-twin, pseudo-twin and 120°-rotational ordered  $\gamma/\gamma$  lamellar interfaces ( $\Gamma_T$ :  $\Gamma_P$ :  $\Gamma_R$ ) has been estimated roughly to be 1: 3: 2 (experimental) or 1: 7: 6 (theoretical) by Inui et al.<sup>[12]</sup>. Fu and Yoo<sup>[17]</sup> have calculated that the energies of the true-twin,



pseudotwin and  $120^\circ$ -rotational ordered  $\gamma/\gamma$  lamellar interfaces in the Ti-50Al alloy are 60, 270 and 250  $\text{mJ}/\text{m}^2$  ( $\Gamma_T : \Gamma_P : \Gamma_R = 1 : 4.5 : 4.2$ ), respectively. Owing to the high interfacial energy, the thermal stability of  $120^\circ$ -rotational ordered interface is poor compared with that of the coherent true twin interface with low interfacial energy. However, the energy of pseudotwin interface is slightly higher than that of  $120^\circ$ -rotational ordered interface but the thermal stability of the former is superior to that of the latter. This phenomenon results from the difference of atomic arrangement across the pseudotwin interface and the  $120^\circ$ -rotational ordered interface.

Fig. 8 shows the schematic illustrations of atomic arrangement on  $\{110\}$  plane across the three types of  $\gamma/\gamma$  lamellar interfaces. The projection direction, the crystal plane, direction indices and the atomic stacking sequence on  $(111)$  plane are denoted in Fig. 8. The atomic stacking sequence on  $(111)$  plane across the pseudotwin interface, which is the same as that across the true twin interface except the symmetric relationship of atom category, is mirror symmetric ( $\dots ACBACBA \dots$ ). While the atomic stacking sequence on  $(111)$  plane across the  $120^\circ$ -rotational ordered interface is invariant ( $\dots CBACBACBA \dots$ ); just the atom categories on specific lattice sites corresponding to the perfect crystal are altered. Hence, the migration of  $120^\circ$ -rotational ordered interface could be simply achieved by thermally activated short-range jumps of atoms in exchanging lattice sites with neighboring atoms. For example, as shown in Fig. 8(c), when the two pairs of neighboring Ti and Al atoms,  $a$  and  $b$  as well as  $c$  and  $d$ , exchange their lattice sites respectively by short-range jumps to neighboring voids, the segment of  $120^\circ$ -rotational ordered interface will migrate. Thermally activated

short-range jumps of atoms during aging at high temperature up to  $1150^\circ\text{C}$ , the migration or dissociation of  $120^\circ$ -rotational ordered interface takes place readily. On the other hand, the mirror symmetrical relationship of atomic stacking sequence on  $(111)$  plane across the true twin and pseudotwin interfaces means that the twin interface migration requires additional integral twinning shear of  $\gamma$  lamella accomplished by the slip of the  $1/6\langle 121 \rangle$  Shockley partial dislocations on  $(111)$  plane. Consequently, the true twin and pseudotwin interfaces are more difficult to migrate or dissociate compared with the  $120^\circ$ -rotational ordered interface.

In addition to the  $120^\circ$ -rotational ordered lamellar interfaces in lamellar microstructure, there are many irregular  $120^\circ$ -rotational ordered  $\gamma$  domain boundaries within a single  $\gamma$  lamella (see Fig. 3(d)). The existence of these  $\gamma$  domain boundaries can degrade the thermal stability of lamellar structure. Although the migration of  $120^\circ$ -rotational ordered  $\gamma$  domain boundaries does not alter the  $\gamma$  lamellar width but merely alters the size of  $\gamma$  domains coexisting within a single  $\gamma$  lamella, the triple point junctions between the  $\gamma$  domain boundaries and the lamellar interfaces act frequently as the initiative positions of lamellar interface dissociation. The  $\gamma$  domain boundaries exert interfacial tensions upon the lamellar interfaces which lead to curvature variation at local lamellar interfaces. Due to the introduction of curvature perturbation into lamellar interfaces, chemical potential gradients are set up according to the Gibbs-Thomson theorem. Diffusion will occur in response to these gradients during aging, then the "thermal groove" at the trip point (shown in Fig. 4 marked by arrow  $G$ ), will form and this process can eventually lead to dissociation of lamellar interfaces. This event is similar to

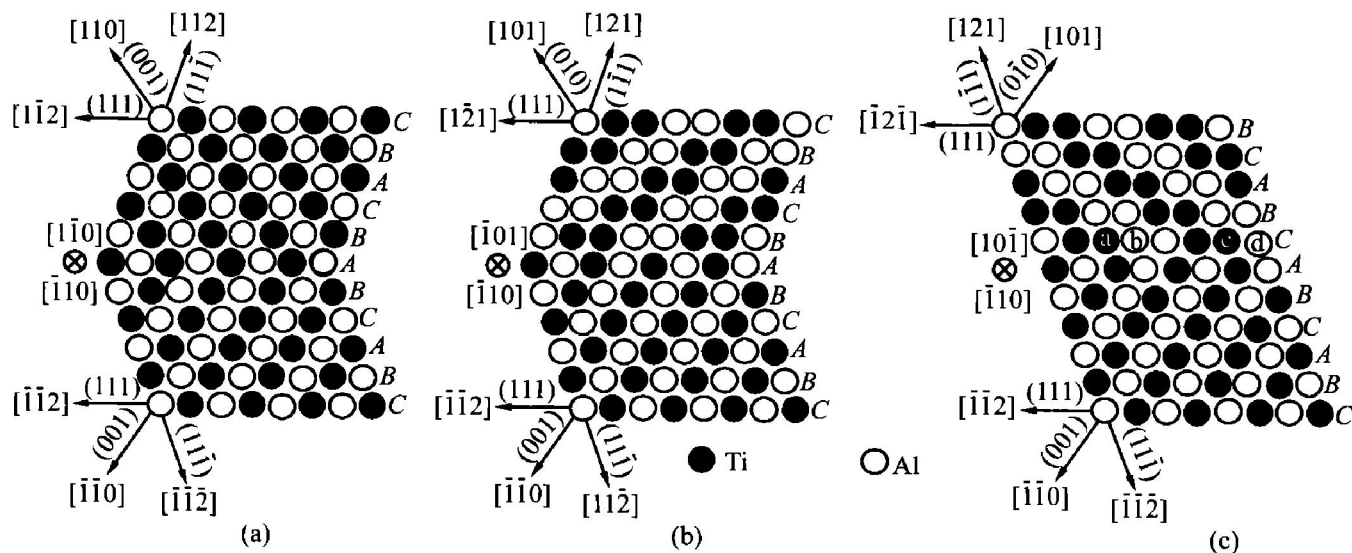


**Fig. 8** Schematic illustrations of atomic arrangement on  $\{110\}$  plane across  $\gamma/\gamma$  lamellar interfaces (a) true twin interface, (b) pseudotwin interface and (c)  $120^\circ$ -rotational ordered interface

the case that sub-boundaries introduced by deformation and recovery processes into a lamellar structure during a thermomechanical process can deteriorate the thermal stability of lamellar structures through the formation of grooves at the triple point junctions between sub-boundaries and lamellar interfaces as described by Nakagawa and Weatherly<sup>[18]</sup>. This process is schematically illustrated in Fig. 7.

## 5 CONCLUSIONS

1) Continuous coarsening of the fully lamellar microstructure in Ti-48Al alloy occurs when aged at 1150 °C. The volume diffusion controlled continuous coarsening can occur not only by migration of interface faults (such as ledges, edges and curved interfaces) but also by migration and decomposition of perfect  $\gamma/\gamma$  lamellar interfaces.

2) During the early stage of aging at 1150 °C, the interface migration and dissociation take place preferentially at the 120°-rotational ordered lamellar interfaces. Comparing the relative thermal stability of the  $\alpha$ -twin,  $\alpha$ -pseudotwin and 120°-rotational ordered  $\gamma/\gamma$  lamellar interfaces shows that the 120°-rotational ordered lamellar interface is the most unstable because of its high interfacial energy and special atomic arrangement.

3) The existence of 120°-rotational ordered  $\gamma$  domain boundaries within  $\gamma$  lamellae can lead to the formation of thermal grooves, which act frequently as the initiative positions of interfacial dissociation, at the triple point junctions between the  $\gamma$  domain boundaries and the lamellar interfaces during aging. Hence, the  $\gamma$  domain boundaries within  $\gamma$  lamellae could degrade the thermal stability of lamellar structure.

## REFERENCES

- [1] Kim Y W. Effects of microstructure on the deformation and fracture of  $\gamma$ -TiAl alloys [J]. *Mater Sci Eng*, 1995, 192/193A: 519 - 533.
- [2] Apple F, Wagner R. Microstructure and deformation of two-phase  $\gamma$ -titanium aluminides [J]. *Mater Sci & Eng*, 1998, R22: 187 - 268.
- [3] Bartholomeusz M F, Wert J A. Modeling creep deformation of a two-phase TiAl/Ti<sub>3</sub>Al alloy with a lamellar microstructure [J]. *Metall Mater Trans*, 1994, 25A: 2161 - 2172.
- [4] Wang J G, Hsiung L M, Nieh T G. Microstructural instability in a creep fully lamellar TiAl alloy [J]. *Intermetallics*, 1999, 7: 757 - 763.
- [5] Ju C P, Fournelle R A. Cellular precipitation and discontinuous coarsening of cellular precipitate in an Al-29at. % Zn alloy [J]. *Acta Metall*, 1985, 33 (1): 71 - 81.
- [6] Kaya M, Smith R W. The discontinuous coarsening reactions in the Pb-Cd and Zr-Cd lamellar eutectic alloys (I): The driving force, initiation and the morphology [J]. *Acta Metall*, 1989, 37 (6): 1657 - 1665.
- [7] Shong D S, Kim Y W. Discontinuous coarsening of high perfection lamellae in titanium aluminides [J]. *Scripta Metall*, 1989, 23(2): 257 - 261.
- [8] Mitao S, Bendersky L A. Coarsening behavior of lamellar structure in Ti-(40-47)Al (at. %) alloy [A]. Kim Y W. *Gamma Titanium Aluminides [C]*. Warrendale, USA: TMS, 1995. 181 - 188.
- [9] Mitao S, Bendersky L A. Morphology and growth kinetics of discontinuous coarsening in fully lamellar Ti-44Al alloy [J]. *Acta Mater*, 1997, 45 (11): 4475 - 4489.
- [10] Jung J Y, Park J K. Growth kinetics of discontinuous coarsening of lamellar structure in Ti-44at. % Al (-0.5at. % Cr) intermetallic compounds [J]. *Acta Mater*, 1998, 46(12): 4123 - 4130.
- [11] Inui H, Nakamura A, Oh M h, et al. High-resolution electron microscopy study of lamellar boundaries in Ti-rich TiAl polysynthetically twinned crystals [J]. *Ultra-microscopy*, 1991, 29: 268 - 278.
- [12] Inui H, Oh M h, Nakamura A, et al. Ordered domains in TiAl coexisting with Ti<sub>3</sub>Al in the lamellar structure of Ti-rich TiAl compounds [J]. *Phil Mag*, 1992, 66(4): 539 - 555.
- [13] Blackburn M J, Jaffee R I, Promisel N E. *The Science Technology and Application of Titanium [M]*. Oxford: Pergamon Press, 1970. 633 - 643.
- [14] Jin Z, Gray III G T. Experimental determination of domain orientations and domain orientation relationships across lamellar interfaces in polysynthetically twinned TiAl crystals [J]. *Mater Sci & Eng*, 1997, A231: 62 - 71.
- [15] Jin Z, Gray III G T. On deformation twins and twin-related lamellae in TiAl [J]. *J Mater Sci*, 1998, 33: 77 - 83.
- [16] Ramanujan R V, Maziasz P J, Liu C T. The thermal stability of the microstructure of  $\gamma$ -based titanium aluminides [J]. *Acta Mater*, 1996, 44(7): 2611 - 2642.
- [17] Fu C L, Yoo M H. Interfacial energies in two-phase TiAl-Ti<sub>3</sub>Al alloy [J]. *Script Mater*, 1997, 37 (10): 1453 - 1459.
- [18] Nakagawa Y G, Weatherly G C. The stability of lamellar structures [J]. *Metall Trans*, 1972, 3(12): 3223 - 3229.

(Edited by PENG Chao-qun)